AFM and Electron Microscopy Study of the Unusual Aggregation Behavior of Metallosurfactants Based on Iron(II) Complexes with Bipyridine Ligands

Paula Garcia,[†] Peter Eaton,[†] Huub P. M. Geurts,[‡] Miguel Sousa,[†] Paula Gameiro,[†] Martin C. Feiters,*[,§] Roeland J. M. Nolte,[§] Eulália Pereira,*[,†] and Baltazar de Castro[†]

REQUIMTE/Departamento de Química, Faculdade de Ciências, Universidade do Porto, Rua do Campo Alegre, 687, 4169-007 Porto, Portugal, and Central Facility for Electron Microscopy, Department of General Instrumentation, and Department of Organic Chemistry, Institute for Molecules and Materials, Radboud University Nijmegen, Toernooiveld, NL-6525 ED Nijmegen, The Netherlands

Received February 26, 2007. In Final Form: May 10, 2007

The aggregation behavior in water-rich solutions of five iron(II) complexes with alkylated derivatives of 2,2′-bipyridine was studied by electron microscopy (cryo-SEM, SEM, and TEM) and AFM. The results obtained by cryo-SEM on frozen colloidal solutions show that the morphology of the aggregates strongly depends on the length of the alkyl chains in the bipyridine ligands, with shorter alkyl chains forming rod-like structures, whereas for compounds with longer alkyl chains, only spherical structures were detected. The self-aggregates were further characterized by SEM and TEM. The results show that their overall morphology depends only on the length of the alkyl chain of the bipyridine ligands and that the samples show a broad size distribution. In addition, TEM and SEM were used to study the stability of the self-aggregates in solution, the effect of addition of methanol, and the temperature used in the preparation of the colloidal solutions. AFM studies of the aggregates either dried in ambient conditions or dehydrated by long drying under vacuum showed partially collapsed self-aggregates in the latter case, showing that the aggregates contain water in their core, indicating that the self-aggregation leads to vesicle-type structures.

Introduction

The attachment of lipophilic carbon chains to ligands followed by complexation with transition metals provides a means of combining amphiphilic properties, such as surface activity and self-assembly, with the physicochemical properties of metal complexes, namely, rich spectroscopic properties, acid−base and redox activity, magnetic properties, etc. Several applications have been proposed for metallosurfactants such as use as probes for magnetic resonance imaging,[1] templates for mesoporous materials,[2,3] as metallomesogens,[4,5] sensitizers for optoelectronic devices,[6−10] homogeneous catalysts,[11−13] and as antihelmintic therapeutics.[14] The affinity of transition metal ions for certain amphiphilic chelating compounds has also been used to promote vesicle formation[15,16] and layer-by-layer film formation.[17] In particular, lipophilic derivatives of 2,2′-bipyridine have been widely used to confer amphiphilic properties on metal complexes,[2,3,6,7,9,10,18−24] with possible catalytic and photophysical applications. Nevertheless, the aggregation behavior of bipyridine-based metallosurfactants is still poorly explored. Many of the studies in the literature report the formation of micelles from metallosurfactants in solution,[25−28] although evidence for inverted vesicles has also been reported.[22]

To evaluate the ability of lipophilic derivatives of 2,2′-bipyridine as building blocks for metal-containing nanoassemblies, we have synthesized and studied the aggregation behavior in water of the complexes $[FeL_2(CN)_2]$ **1**−**5** (**1**, L = 4,4′-dipentyl-

* Corresponding authors. (M.C.F.) Fax: +31 24 365 2929; tel.: +31243652016; e-mail: m.feiters@science.ru.nl. (E.P.) Fax: +351 22 6082 959; tel.: +351 22 6082 888; e-mail: efpereir@fc.up.pt.

[†] Universidade do Porto.

[‡] Central Facility for Electron Microscopy, Department of General Instrumentation, Radboud University Nijmegen.

[§] Department of Organic Chemistry, Institute for Molecules and Materials, Radboud University Nijmegen.

(1) Binnemans, K.; Gorller-Walrand, C. *Chem. Rev.* **2002**, *102*, 2303−2345.

(2) Jervis, H. B.; Raimondi, M. E.; Raja, R.; Maschmeyer, T.; Seddon, J. M.; Bruce, D. W. *Chem. Commun.* **1999**, 2031−2032.

(3) Danks, M. J.; Jervis, H. B.; Nowotny, M.; Zhou, W. Z.; Maschmeyer, T. A.; Bruce, D. W. *Catal. Lett.* **2002**, *82*, 95−98.

(4) Donnio, B. *Curr. Opin. Colloid Interface Sci.* **2002**, *7*, 371−394.

(5) Serrano, J. L.; Sierra, T. *Coord. Chem. Rev.* **2003**, *242*, 73−85.

(6) Nazeeruddin, M. K.; Zakeeruddin, S. M.; Lagref, J. J.; Liska, P.; Comte, P.; Barolo, C.; Viscardi, G.; Schenk, K.; Graetzel, M. *Coord. Chem. Rev.* **2004**, *248*, 1317−1328.

(7) Chu, B. W. K.; Yam, V. W. W. *Inorg. Chem.* **2001**, *40*, 3324−3329.

(8) Tse, C. W.; Lam, L. S. M.; Man, K. Y. K.; Wong, W. T.; Chan, W. K. *J. Polym. Sci., Part A: Polym. Chem.* **2005**, *43*, 1292−1308.

(9) Romualdo-Torres, G.; Agricole, B.; Mingotaud, C.; Ravaine, S.; Delhaes, P. *Langmuir* **2003**, *19*, 4688−4693.

(10) Terasaki, N.; Akiyama, T.; Yamada, S. *Langmuir* **2002**, *18*, 8666−8671.

(11) Qiu, L. G.; Xie, A. J.; Shen, Y. H. *J. Mol. Catal. A: Chem.* **2006**, *244*, 58−63.

(12) Bhattacharya, S.; Snehalatha, K.; Kumar, V. P. *J. Org. Chem.* **2003**, *68*, 2741−2747.

(13) Jiang, F.; Jiang, B. Y.; Cao, Y. S.; Meng, X. G.; Yu, X. Q.; Zeng, X. C. *Colloids Surf., A* **2005**, *254*, 91−97.

(14) Walker, G. W.; Geue, R. J.; Sargeson, A. M.; Behm, C. A. *Dalton Trans.* **2003**, 2992−3001.

(15) Luo, X. Z.; Miao, W. G.; Wu, S. X.; Liang, Y. Q. *Langmuir* **2002**, *18*, 9611−9612.

(16) (a) Song, A.; Jia, X.; Teng, M.; Hao, J. *Chem.−Eur. J.* **2007**, *13*, 496−501. (b) Wang, J. Z.; Song, A. X.; Jia, X. F.; Hao, J. C.; Liu, W. M.; Hoffmann, H. *J. Phys. Chem. B* **2005**, *109*, 11126−11134. (c) Hao, J.; Song, A.; Wang, J.; Chen, X.; Zhuang, W.; Shi, F.; Zhou, F.; Liu, W. *Chem.−Eur. J.* **2005**, *11*, 3936−3940. (d) Hao, J.; Wang, J.; Liu, W.; Abdel-Rahem, R.; Hoffmann, H. *J. Phys. Chem. B* **2004**, *108*, 1168−1172.

(17) Blasini, D. R.; Flores-Torres, S.; Smilgies, D. M.; Abruna, H. D. *Langmuir* **2006**, *22*, 2082−2089.

(18) Holder, E.; Marin, V.; Alexeev, A.; Schubert, U. S. *J. Polym. Sci., Part A: Polym. Chem.* **2005**, *43*, 2765−2776.

(19) Garcia, P.; Marques, J.; Pereira, E.; Gameiro, P.; Salema, R.; de Castro, B. *Chem. Commun.* **2001**, 1298−1299.

(20) Tollner, K.; Popovitz Biro, R.; Lahav, M.; Milstein, D. *Science* **1997**, *278*, 2100−2102.

(21) Soyer, H.; Mingotaud, C.; Boillot, M. L.; Delhaes, P. *Langmuir* **1998**, *14*, 5890−5895.

(22) Dominguez-Gutierrez, D.; Surtchev, M.; Eiser, E.; Elsevier, C. J. *Nano Lett.* **2006**, *6*, 145−147.

(23) Kobayashi, K.; Sato, H.; Kishi, S.; Kato, M.; Ishizaka, S.; Kitamura, N.; Yamagishi, A. *J. Phys. Chem. B* **2004**, *108*, 18665−18669.

(24) Taniguchi, M.; Ueno, N.; Okamoto, K.; Karthaus, O.; Shimomura, M.; Yamagishi, A. *Langmuir* **1999**, *15*, 7700−7707.

10.1021/la700560y CCC: $37.00
Published on Web 06/15/2007 PAGE EST: 6.2

Scheme 1. Chemical Structure of Compounds Studied[a]

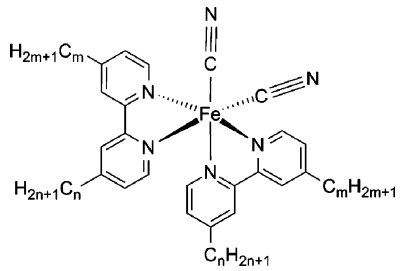

[a] **1**: $m = n = 5$; **2**: $m = n = 7$; **3**: $m = 7$, $n = 1$; **4**: $m = n = 9$; and **5**: $m = n = 13$.

2,2′-bipyridine; **2**, L = 4,4′-diheptyl-2,2′-bipyridine; **3**, L = 4-heptyl-4′methyl-2,2′-bipyridine; **4**, L = 4,4′-dinonyl-2,2′-bipyridine; and **5**, L = 4,4′-bis(tridecyl)-2,2′-bipyridine; Scheme 1). Aggregation of **1**−**5** was first detected in water−methanol, water−acetone, and water−acetonitrile solutions, where a sharp decrease in λ_{max} of the MLCT band in conjunction with an increase in light scattering was observed for water-rich solutions.[29] These complexes are known to be strongly solvatochromic, and the spectral changes observed can be related to the existence of a lipophilic microenvironment around the metal center.[29,30] The lipophilic microenvironment is a strong indication that the compounds aggregate in water-rich solutions. In all cases, these aggregates were stable for at least several months without any evidence of precipitation. In a preliminary communication, we reported the results obtained by TEM and dynamic light scattering for **4**, which revealed the formation of spherical aggregates with diameters ranging from 200 to 500 nm.[19]

In the present paper, we report a TEM, SEM, and AFM study on the morphology of the aggregates of the complexes [$FeL_2(CN)_2$] **1**−**5** in water and in water−methanol mixtures.

Experimental Procedures

The complexes were prepared using a published procedure with minor modifications,[19,29,31] affording **1**−**5** in a cis configuration. For **3**, a mixture of the cis and trans isomers relative to the heptyl chains was used since it was not possible to separate the isomers using standard separation methods. The aggregates were obtained by injecting 50 μL of a methanol solution of the desired compound (10^{-3} M) into 10 mL of an aqueous solution at 65 °C, under Ar bubbling, with stirring. After injection, the solution was maintained at 65 °C for 5 min with Ar bubbling for organic solvent elimination. To study the temperature effect, samples were prepared by the same procedure but the time that the solution was kept at 65 °C was varied. In addition, other samples were prepared using the same procedure at room temperature. In all cases, after cooling to room temperature, ca. 10 μL aliquots were removed for the microscopy studies either immediately (fresh samples), after 24 h, or after 1 week. The solution was deposited in the material used as a support (TEM: Formvar-coated copper grids, 200 mesh; SEM: glass slides coated with Au/Pd by sputtering; and AFM: freshly cleaved mica) and dried at room temperature, and normal pressure, except otherwise stated. For the cryo-SEM studies, samples were used as prepared. TEM was carried out in a JEOL-TEM 1010 microscope, operating at 60 KeV, without the addition of a contrast agent since the presence of the metal ion provided enough contrast. SEM was carried out in a JEOL FEG-SEM (JSM-6330F) microscope, operating at 3 keV, WD = 8 mm. Cryo-SEM was carried out on the same instrument used for conventional SEM with an Oxford Cryo-transfer system CT1500 HF; the sample was rapidly frozen in nitrogen slush at −220 °C, fractured in the cooling pre-chamber of the microscope at −120 °C, subjected to Au/Pd sputtering (1.5 nm), and transferred to the microscope chamber, where it was maintained at −120 °C. All solutions for AFM were prepared using ultrapure pre-filtered water (18 MΩ water for molecular biology, Sigma), to avoid contamination. Samples were examined using a Molecular Imaging PicoLE atomic force microscope in tapping mode. Rectangular silicon cantilevers of a resonant frequency of 75−155 kHz and nominal tip radius <10 nm (MikroMasch) were used.

Results

Electron Microscopy Study of Freshly Prepared Samples. The compounds studied are insoluble in water, even at high temperature, while stirring and sonicating. Nevertheless, stable colloidal solutions could be obtained by the addition of water to a methanol solution of the compound or by injection of a small volume of a methanol solution of the desired compound, into water at 65 °C, with stirring under argon. This injection method is commonly used in the preparation of phospholipid vesicles.[32,33] Formation of aggregates was immediately perceived by a color change from red (monomer) to blue (aggregates). This color change is due to the solvatochromic properties of the present compounds, and it is related to a change in the microenvironment of the iron(II) center from hydrophilic to hydrophobic.[29,30]

The morphological properties of the aggregates formed by the present complexes were studied by SEM, TEM, and cryo-SEM. The cryo-SEM technique allows a direct visualization of the aggregates formed in solution since in this case the images are obtained from samples that are rapidly frozen, then fractured in the frozen state to expose a fresh surface, and subsequently subjected to partial sublimation of the vitreous ice matrix to expose any structures present in solution. In all cases, the results obtained by cryo-SEM were similar to those obtained by SEM and TEM, showing that the aggregates observed by SEM and TEM are present in solution and that no drying artifacts occur during application of these techniques. SEM images of freshly prepared samples of the complexes are shown in Figure 1. The length of the alkyl chains in 2,2′-bipyridine seems to be a key structural factor for the morphology of the aggregates. Compound **1** (Figure 1A), with four five-carbon chains, formed rod-like aggregates with average lengths that varied considerably from sample to sample, viz. from 650 to 3500 nm, and widths that varied within the range of 60−150 nm. Cryo-SEM images showed the same type of rod-like aggregates, some of them protruding from the surface (Figure 2A, black arrows). In addition to the rod-like structures, cryo-SEM images showed some large sheet-like aggregates (Figure 2A, gray arrow) and some disrupted films lying on the surface (Figure 2A, white arrow), possibly resulting from unaggregated compounds that remained after solvent evaporation.

SEM images for **2** (Figure 1B) with four seven-carbon chains also showed rod-like aggregates, although with a lower average aspect ratio (length range of 65−430 nm, width range of 45−170 nm), as well as spherical aggregates (diameter range of 20−220 nm). In this case, the individual structures were clustered

(25) Bowers, J.; Amos, K. E.; Bruce, D. W.; Heenan, R. K. *Langmuir* **2005**, *21*, 5696−5706.
(26) Bowers, J.; Amos, K. E.; Bruce, D. W.; Webster, J. R. P. *Langmuir* **2005**, *21*, 1346−1353.
(27) Bowers, J.; Danks, M. J.; Bruce, D. W. *Langmuir* **2003**, *19*, 292−298.
(28) Bowers, J.; Danks, M. J.; Bruce, D. W.; Webster, J. R. P. *Langmuir* **2003**, *19*, 299−305.
(29) Gameiro, P.; Pereira, E.; Garcia, P.; Breia, S.; Burgess, J.; de Castro, B. *Eur. J. Inorg. Chem.* **2001**, 2755−2761.
(30) Pereira, E.; Garcia, P.; Breia, S.; Maia, A.; Gameiro, P.; de Castro, B. *Biophys. J.* **2001**, *80*, 374a.
(31) Schilt, A. A. *J. Am. Chem. Soc.* **1960**, *82*, 3000−3005.
(32) Cuccovia, I. M.; Schroter, E. H.; Baptista, R. C. D.; Chaimovich, H. *J. Org. Chem.* **1977**, *42*, 3400−3403.
(33) New, R. R. C. *Liposomes—A Practical Approach*; Oxford University Press: Oxford, 1990.

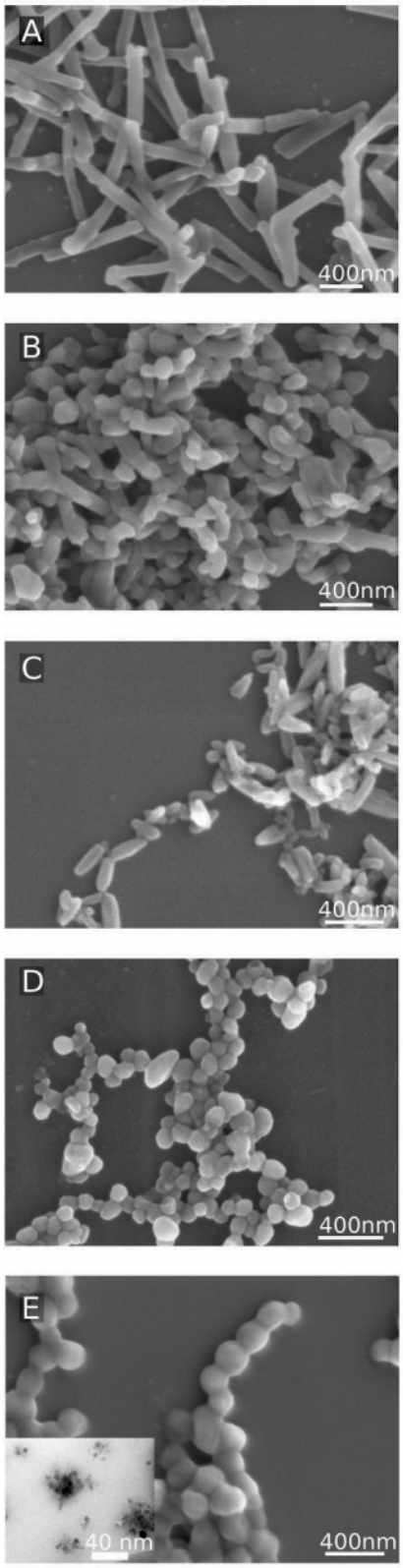

Figure 1. SEM micrographs of freshly prepared samples of **1** (A), **2** (B), **3** (C), **4** (D), and **5** (E). The inset of panel E is a higher magnification image showing the smaller features observed in this sample.

in a three-dimensional network both in frozen solution (cryo-SEM, Figure 2B) and in dehydrated samples (SEM, Figure 1B).

Compound **3**, with one seven-carbon chain and one methyl group on each ligand (Figure 1C), showed a homogeneous population of elongated aggregates, but in this case, the structures are wider in the middle than at the ends, resembling rice grains

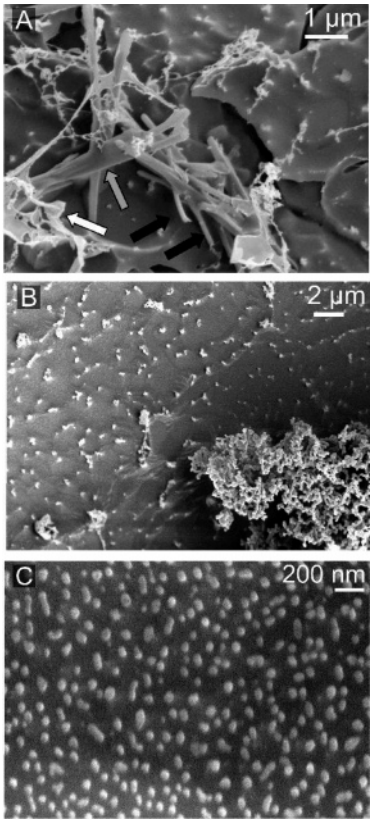

Figure 2. Cryo-SEM micrographs of freshly prepared samples of **1** (A), **2** (B), and **4** (C). For explanation of the arrows, see text.

(length range of 65−430 nm, range of widths at the middle of 40−170 nm).

Compound **4** (Figures 1D and 2C), with four nine-carbon chains, showed only spherical aggregates with diameters in the range of 30−270 nm. These aggregates were partially clustered in the SEM samples probably due to the dehydrating conditions of the sample since in freshly prepared frozen samples studied by cryo-SEM, no clusters were observed.

Compound **5** showed only spherical aggregates, but two different populations were observed: aggregates with diameters in the range of 5−10 nm (Figure 1E, inset) and aggregates with a mean diameter of ≈120 nm (Figure 1E).

Except for the 5−10 nm aggregates observed for **5**, all the other aggregates detected have dimensions that exclude the possibility of micellar structures since such structures usually have radii on the order of magnitude of the length of the extended molecule.[33,34] The range of sizes observed is typical for vesicle-like aggregates. This means that they should have an aqueous core, which can be easily detected by simple encapsulation experiments using a strongly hydrophilic fluorescent probe, such as 5(6)-carboxyfluorescein.[33] This assay is commonly used to probe the formation of vesicles in phospholipid suspensions and is based on the strong auto-quenching effect of the probe. Samples were prepared as usual but using a 1 M aqueous solution of 5(6)-carboxyfluorescein instead of pure water. At this concentration, fluorescence of the probe is low due to auto-quenching. After checking the formation of the aggregates by UV−vis spectroscopy, the aggregates were separated from the free probe by size exclusion chromatography (Sephadex G50). The presence of an aqueous core in the aggregates may be ascertained by checking the fluorescence intensity of the sample after separation,

(34) Jönsson, B.; Holmberg, B. L. K.; Kronberg, B. *Surfactants and Polymers in Aqueous Solution*; John Wiley and Sons: New York, 1998.

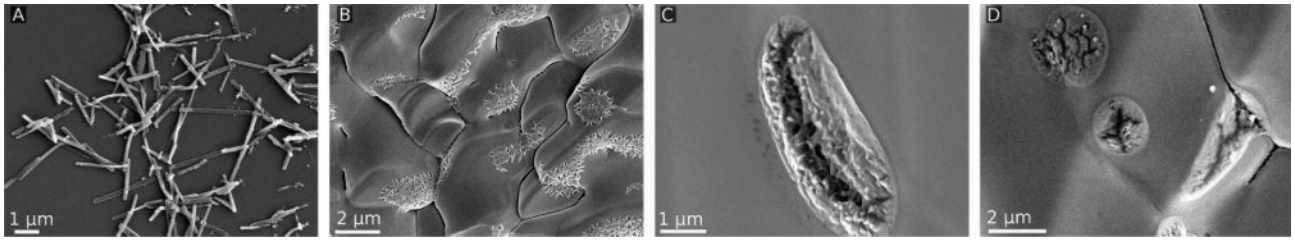

Figure 3. (A) SEM image of a sample of **1** after 1 day in solution; (B and C) cryo-SEM micrographs of a sample of **2** after 9 days in solution; and (D) cryo-SEM micrograph of a sample of **4**, after 9 days in solution.

with and without the addition of a vesicle disruption agent (e.g., Triton X100). If the fluorescence intensity increases drastically after the addition of Triton X100, then an aqueous core must have been present in the aggregates since the addition of Triton X100 releases the fluorescent probe to the bulk solution, decreasing its concentration and thus the auto-quenching effect. For all the complexes studied, a strong increase in fluorescence was observed after adding Triton X100 (increase of 2−20 times), showing that the hydrophilic probe remained trapped inside an aqueous core. It should be noted that for **5**, as for the other complexes, only one fraction was detected that displayed fluorescence after treatment with Triton X100, in spite of the observation by microscopy of two different populations of very different sizes. Since the elution volumes of the fractions for **4** and **5** were very similar, the fluorescent fraction for **5** was ascribed to the 120 nm aggregates.

Electron Microscopy Study of Aged Samples. In all cases, the individual aggregates, once formed, showed a strong tendency toward clustering or fusion in solution at room temperature, and after a few days at room temperature, larger fused or clustered structures were observed, depending on the compound. Fusion was the main process for **1**, while clustering seemed to be the prevailing process for all the other compounds studied. Figure 3A shows an SEM image obtained for a sample of **1**, 1 day after preparation. The morphology of the aggregates in the sample was similar to that observed for freshly prepared samples, but there was a marked increase in the average length and in the average width, showing that fusion was a non-directional process. In contrast, **2** and **4** displayed mainly clustering of the formed aggregates. Cryo-SEM images of samples of **2**, 9 days after preparation, showed the formation of microdomains formed by aggregation of rod-like structures (Figure 3B,C) that in some cases were surrounded by a film. Some of these latter structures were broken (probably as a result from the cryo-fracturing of the samples), showing a core containing rod-like aggregates (Figure 3C). In both types of structures, the individual rod-like aggregates showed a marked increase in their length (length determined by SEM of 200 nm to 1 μm), indicating that fusion also contributed to the aging process of the aggregates. Studies on aged samples of **4** showed that the formation of clusters of spherical particles was a faster process, and after 1 day in solution, the majority of the spherical aggregates had become clustered in solution. After 9 days in solution, the only structures detected by cryo-SEM (Figure 3D) were microdomains with an average length of ≈4 μm surrounded by a film. Some of these spherical or oval-shaped microdomains were broken and revealed a core made up of individual spherical aggregates.

Effect of Incubation Time and Solvent. The incubation time at 65 °C and the amount of methanol are also important factors that influence the properties of the aggregates. SEM images of samples prepared by the same method at room temperature and at 65 °C but limiting the incubation period at the latter temperature to less than 2 min showed only irregular structures with diameters of 100−200 nm for all the compounds studied. For incubation

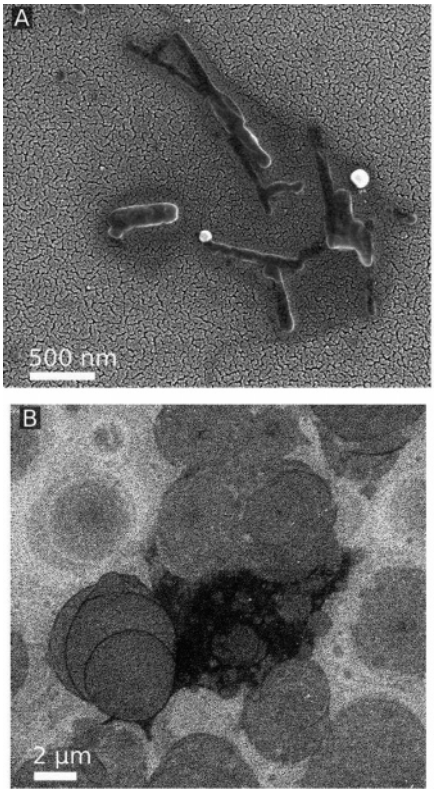

Figure 4. SEM micrographs of samples of (A) **1** with addition of 5% (v/v) methanol and (B) **4** with addition of 75% (v/v) methanol.

periods at 65 °C of 5−15 min, formation of rod-like structures was observed for **1**−**3**, while for the other compounds studied, the aggregates maintained their spherical morphology but became much more regular and attained smoother surfaces. For the compounds that formed rod-like structures, the average length of the rods increased with the incubation time. For the 15 min incubation samples, some clustering of the structures was detected, but for longer incubation periods, the number of aggregates detected in the sample decreased, and most of the sample was composed of irregular films.

The effect of adding methanol was studied for methanol concentrations of 0.5−25% (v/v). The addition of this solvent was performed both before and after incubation at high temperature, and the results were similar. For all the compounds studied, increasing amounts of methanol caused a decrease of the stability of the aggregates relative to the dehydrating conditions of the SEM experiments. Figure 4A shows a typical picture of a sample of **1** containing 5% methanol, where clearly some of the aggregates are partially collapsed. For larger amounts of methanol, more collapsed structures were observed. In addition, the remaining aggregates showed an irregular surface, in contrast to what was observed in water where all the aggregates showed a smooth surface. With 10−75% methanol present in solution, the samples in all cases showed large round films with average

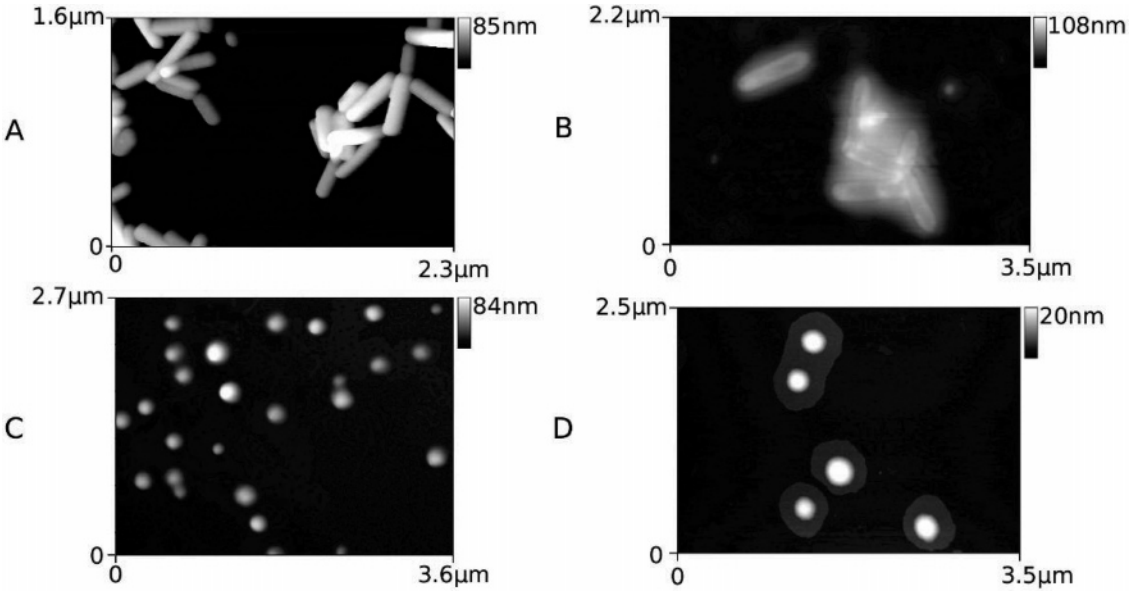

Figure 5. AFM images of vesicles formed from **1** imaged after air drying on the mica substrate (A) and after vacuum drying (B) and **4** imaged after drying in air (C) and under vacuum (D).

Table 1. Average Vesicle Dimensions as Measured by AFM, TEM, and SEM[a]

	compound 1			compound 4
	length (nm)	width (nm)	aspect ratio	width (nm)
AFM	380−700	60−80	6.0−9.0	40−55
TEM	660−940	70−125	5.0−10.0	50−100
SEM	1200−1700	120−150	9.0−12.0	80−130

[a] Values are the range of averages for different batches (at least 20 measurements per batch). Widths as reported from AFM measurements were measured from vesicle heights (see text).

diameters of 2−5 μm (Figure 4B). These films showed a darker exterior boundary, indicating that they were probably formed by the collapse of large vesicle-type structures. Similar structures were also seen for those compounds that formed rod-like aggregates in water. The amount of methanol necessary to induce these changes was found to be lower for the longer alkyl chain samples. For example, complex **4** in methanol/water 1% v/v (or higher amounts of methanol) formed mainly large vesicles with diameters of 0.5−3 μm, in agreement with our previously reported TEM images.[19]

AFM Study. To gain insight into the 3-D structure of the aggregates, AFM was carried out. Compounds **1** and **4** were selected for this study because they were representative of the different morphologies observed (i.e., rod-like and spherical, respectively). AFM images of aggregates prepared from **1** and **4** are shown in Figure 5A,C, respectively. Both samples were dried under ambient conditions. The structures of the aggregates were quite similar to those observed by cryo-SEM, SEM, and TEM. Table 1 shows that the dimensions of the aggregates as measured by the TEM, SEM, and AFM techniques are quite similar, although the variation between batches was quite large. In general, the height as measured by AFM was somewhat smaller than the width as measured by TEM or SEM. TEM shadowing experiments (not shown) showed that the rod width and rod heights were the same for individual rods. Quantitative measurement of the width of such high-aspect ratio features by AFM is not possible, however, due to convolution of the sample topography with the shape of the tip.[35]

In some, but not all cases, further dehydration of the samples of **1** and **4** by vacuum desiccation led to aggregates with a considerably different morphology. Two such images of dehydrated aggregates are shown in Figure 5B (compound **1**) and Figure 5D (compound **4**). Figure 5B shows the typical rods of the pentyl modified compound but with a distinctive flattened morphology. In addition, the rods are surrounded by some collapsed material. This effect was seen several times for dehydrated aggregates, although it did not always occur. In addition, it was possible to observe intact aggregates as well as flattened aggregates in the same sample. However, this flattened morphology was never seen unless the samples had been vacuum dried. Figure 5D shows that the aggregates of **4** were also strongly affected by drying. These vacuum dried aggregates appeared broader and flatter than those dried under ambient conditions (Figure 5C). Furthermore, each aggregate was surrounded by a broad plateau, which was 2.6 nm (standard deviation 0.2 nm) high. Again, this effect was only seen for some aggregates after vacuum drying but never for aggregates prepared under ambient conditions.

Discussion

The aggregation behavior observed for the compounds studied in this work is typically that of amphiphilic molecules, containing a hydrophilic headgroup and a hydrophobic tail. These molecules form self-assembled structures in water, to maximize the interactions of the hydrophilic part with the solvent, while minimizing the contact of the hydrophobic part with the solvent. In the case of **1**−**5**, the alkyl chains are obviously hydrophobic, as are also the bipyridine ligands,[36] which can also interact with each other by $\pi-\pi$ stacking. The known solvatochromism of $[Fe(bpy)_2(CN)_2]$ and related alkyl-substituted species, which is the result of hydrogen bonding of the cyanide ligands to protic solvents,[29,30] is evidence of the hydrophilicity of the highly polar $Fe(II)(CN)_2$ moiety in **1**−**5** despite the fact that this moiety has no net charge and does not dissociate into ions. The absence of any charge repulsion combined with the overall high hydrophobicity, including both the alkyl and the bipyridine moieties, explains the self-assembly in water of **1**−**3**, despite the fact that

(35) Gibson, C. T.; Watson, G. S.; Myhra, S. *Wear* **1997**, *213*, 72−79.

(36) Oszwaldowski, S.; Marchut, D. *Anal. Chim. Acta* **2005**, *540*, 207−219.

they contain only short alkyl tails. Nevertheless, it should be noted that the difference in lipophilicity between **1** and the same compound with 4-methyl-4′-pentyl-2,2′-bipyridine ligands is sufficient to make the latter compound water soluble.[30]

To understand the self-assembly behavior of the present compounds, it is useful to compare their structural features and behavior with those of previously reported ruthenium complexes of the general formula $[Ru(bpy)_2(4,4'\text{-}R_2bpy)]^{2+}$, where R is 12 or 19 carbon alkyl chains,[25,27] and $[Ru(bpy)(4,4'\text{-}R_2bpy)_2]^{2+}$, where R is heptadecyl alkyl.[22] The first type of ruthenium complex forms spherical micelles in water with headgroup areas around 100 Å^2, as shown by small angle neutron scattering. The second type of ruthenium complexes yields spherical inverted micelles and spherical inverted vesicles in hexane and toluene, respectively.[22] It should be noted that the molecular structure of this latter complex is more comparable to the present complexes since the number of substituted bipyridine ligands per molecule is in both cases 2, whereas for complex $[Ru(bpy)_2(4,4'\text{-}R_2bpy)]^{2+}$, the number of substituted bipyridine ligands is one per molecule. This difference in molecular structure is expected to have a strong influence on the molecular aggregation of the compounds, leading to a higher volume of the metal complex moiety of the molecules. Taking into consideration the geometrical considerations proposed by Israelachvili[37] for surfactant self-assembly, the limiting chain length for micelle formation in the case of compounds containing two substituted bipyridine ligands is expected to be higher than for compounds with one bipyridine ligand per molecule. For the Fe-bpy surfactants studied here, this would explain the observation of aggregates with dimensions typical of micelles only in the case of **5**, with the longer alkyl chains.

The size exclusion experiments with the fluorescent probe show that in all cases, the aggregates contain encapsulated solvents, and the AFM results indicate that extensive drying of the samples results in flattened structures. The presence of a solvent core is not apparent from the TEM images, but it is not expected to be detected there because of the strong scattering of the electrons by the metal ions in the surfactants. Thus, it seems that water is present inside the aggregates, which is important to keep their spherical or rod-like morphology. The 2.6 nm plateau that surrounds the collapsed aggregates of **4** has a mean thickness close to that expected for one bilayer (as based on a simple CPK model that predicts an extended length of 1.7 nm for this compound). The difference between the measured value (2.6 nm) and the theoretical bilayer thickness (3.4 nm) may imply some interdigitation or tilting of the molecules in the bilayer. We undertook powder X-ray diffraction studies on the dried material, expecting not only to obtain further evidence for the formation of bilayers but also to determine the bilayer thicknesses and relate them to the molecular structures. Unfortunately, the diffraction patterns showed only weak and broad peaks, and no set of peaks that could be assigned to a lamellar packing of stacked bilayers was observed. This result may be due either to very small domain sizes or to a large disorder in the aggregated state and thus does not completely exclude the formation of structures based on regular stacked bilayers. As bilayer thicknesses could not be obtained, it was not possible to draw any conclusions with respect to the effect of the number and length of the alkyl tails on the molecular packing of the compounds.

In the AFM experiments, we were able to study the effect of dehydration on the structure of the aggregates. Since the TEM and SEM pictures were taken under high vacuum, we could not perform such experiments. Nevertheless, the intriguing question

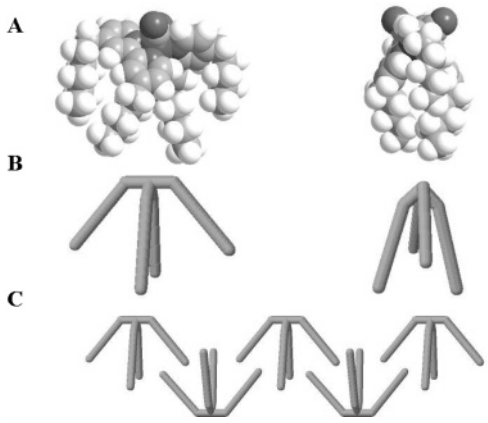

Figure 6. (A) Representations of the molecular structure of **1** obtained by minimization of steric energy (MM2 ChemBats3D 10.0). (B) Schematic representations of the molecular structure corresponding to each of the views in panel A. (C) Schematic representation of possible molecular aggregation.

remains as to why the TEM and SEM images more closely resemble the AFM images of hydrated vesicles than those of the dehydrated vesicles. That is, why were the vesicles as observed by SEM and TEM not surrounded by the material seen in the AFM images of dehydrated vesicles? One possible explanation is that the present compounds have a higher affinity for the support used in the AFM studies (mica) than for the support used in the TEM and SEM studies (Formvar and glass, respectively).

Another important experimental observation requiring an explanation is the unusual rod-like aggregation observed for the short chain amphiphiles **1**−**3**. Self-assembly into tubules, rods, and fibers is usually restricted to cases where the driving force for assembly is some directional intermolecular interaction, such as hydrogen bonding, and $\pi-\pi$ stacking.[38−40] Although for **1**−**5** the existence of $\pi-\pi$ stacking between bipyridine ligands on neighboring molecules may not be ruled out completely, the cis configuration around the metal center and the steric hindrance of the alkyl groups at the positions 4 and 4′ of these ligands make this type of interaction very unlikely. In addition, a question that remains open is why the directional interaction between molecules is not expressed in the case of the aggregates of the compounds with longer alkyl chains (i.e., compounds **4** and **5**). A possible explanation relies on the asymmetric molecular structure imposed by the coordination center, schematically represented in Figure 6. It is possible that, as the length of the alkyl chain increases, the asymmetry induced by the molecular shape of the metal complex headgroup will be lost due to the higher efficiency of the longer chains to occupy void spaces, leading to a less rigid aggregation.

The results obtained in the experiments at different aggregation intervals show that all aggregates have a strong tendency to fuse into larger structures. This behavior is typical of neutral surfactants, but the presence of four alkyl chains per molecule may also play a role. In fact, simulation studies on the aggregation behavior of single- and double-tail surfactants indicate that, by increasing the number of lipophilic tails, the ability of the headgroup to shield the hydrophobic tails from the solvent becomes weaker.[41] This inability to shield the tails introduces

(37) Israelachvili, J. N.; Mitchell, D. J.; Ninham, B. W. *J. Chem. Soc., Faraday Trans.* **1976**, *72*, 1525−1568.

(38) Sommerdijk, N. A. J. M.; Buynsters, P. J. A. A.; Pistorius, A. M. A.; Wang, M.; Feiters, M. C.; Nolte, R. J. M.; Zwanenburg, B. *J. Chem. Soc., Chem. Commun.* **1994**, 1941−1942.

(39) Sommerdijk, N. A. J. M.; Feiters, M. C.; Nolte, R. J. M.; Zwanenburg, B. *Recl. Trav. Chim. Pays-Bas* **1994**, *113*, 194−200.

(40) Sommerdijk, N. A. J. M.; Lambermon, M. H. L.; Feiters, M. C.; Nolte, R. J. M.; Zwanenburg, B. *Chem. Commun.* **1997**, 455−456.

(41) Shillcock, J. C.; Lipowsky, R. *J. Chem. Phys.* **2002**, *117*, 5048−5061.

some disorder in the molecular aggregates because the solvent becomes inserted into the lipid cores, increasing the driving force for aggregation/fusion.

The behavior of the aggregates upon addition of increasing concentrations of methanol is also typical of amphiphilic compounds. It is well-known from experimental and computational studies that the addition of methanol to amphiphilic aggregates decreases the bilayer thickness because it induces interdigitation of the tails and hence fusion events.[42] These effects have been attributed to the fact that the alcohol molecules become located at the hydrophilic/hydrophobic interface, which increases the average headgroup area, and to a decrease of the interfacial tension as a result of the increase in alcohol concentration in the bulk solvent.

Taken together, our results suggest that self-assembly of **1**−**5** is a kinetically driven process and that the thermodynamically stable morphology of the aggregates in all cases is the bilayer-based structures observed in aged samples, either in the form of large vesicles and rod-like structures or as films.

Acknowledgment. We thank Fundação para a Ciência e Tecnologia (FCT) for financial support through Contract POCTI/QUI/38605/2001. P.G. thanks FCT for Grant PRAXIS XXI/BD/15922/98. P.E. thanks FCT for Grant SFRH/BPD/17617/2004. We thank Laboratório de Química Analítica, Faculdade de Ciências, Universidade do Porto for the use of the AFM microscope.

LA700560Y

(42) Patra, M.; Salonen, E.; Terama, E.; Vattulainen, I.; Faller, R.; Lee, B. W.; Holopainen, J.; Karttunen, M. *Biophys. J.* **2006**, *90*, 1121−1135.